A Criticality Safety Analysis of PWR Spent Fuel Storage Pool with Burnup Credit and Axial Burnup Profile

Kyu Jung Choi, Ye Seul Cho, Ser Gi Hong*
Department of Nuclear Engineering, Kyung Hee University, 1732 Deogyeong-daero, Giheung-gu, Yongin-si, Gyeonggi-do, 17104, Republic of Korea
**Corresponding author: sergihong@khu.ac.kr*

1. Introduction

In our country, all of the PWR spent fuel assemblies have been stored in the spent fuel pool storage inside the reactor building but the statistics of the spent fuel generation and storage show that most of the spent fuel pool storage will be saturated in the near future. So, the dry storage of PWR spent fuels should be considered for resolving the spent fuel issue. Also, the design of the dense spent fuel storage racks should be considered before the dry storage of PWR spent fuels and therefore the criticality safety analysis for the spent fuel storage pool is very important. We considered the discharged fuel assemblies from the 6th cycle core of Hanbit Unit 3. The purpose of this work is to give the detailed criticality analysis of a PWR spent fuel storage pool with consideration of burnup credit and realistic axial burnup profiles and to evaluate the loading curves for various cooling times.

2. Methods and Results

2.1 Description of spent fuel storage racks and axial burnup profiles

The typical PWR spent fuel storage pools consist of two regions (i.e., Region I, Region II). The discharged fuel assemblies from the reactor core are first moved into the Region I and they are stored here, and then they are moved into the Region II and stored there before they are moved for the interim dry storage or for final repository. Therefore, the fuel assemblies have lower reactivity in Region II than in Region I due to decays of the fission products and fissile nuclides (the most dominant actinide is Pu-241 due to its short half-life). The figures 1 and 2 show the configurations of the storage racks of Regions I and II, respectively. The spent fuel storage racks of Region I have the inter-cell flux trap gaps which are composed of stainless steel and water to reduce the reactivity while the ones of Region II have no inter-cell flux trap gap due to lower reactivity due to the cooling. Our preliminary calculations showed that the unit geometry cell with radial reflective boundary conditions for the Region I storage rack (given in Fig. 1) has sufficiently low k_{eff} even without the burnup credit application. Therefore, in this work, we performed the criticality analysis only for Region I.

Table I summarizes the main specifications of the unit cell for the spent fuel storage racks.

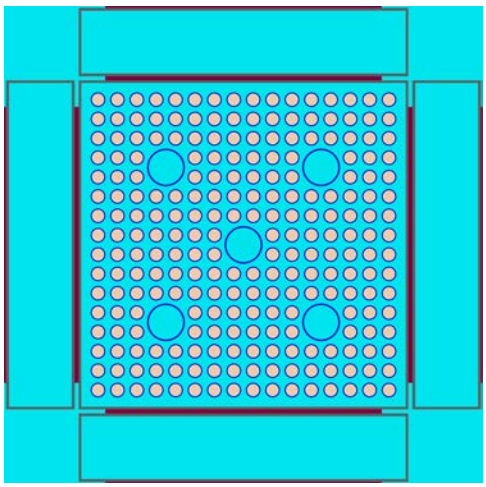

Fig. 1. Configuration of the Region I storage rack.

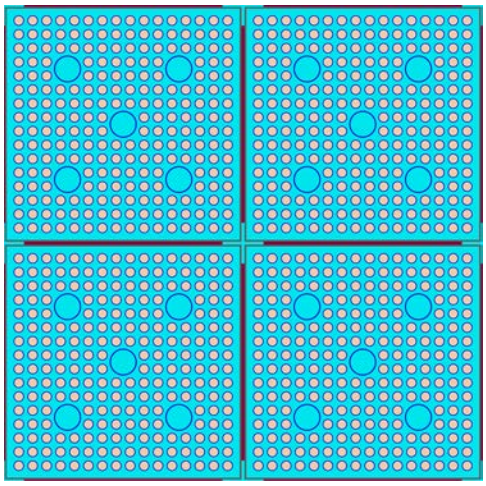

Fig. 2. Configuration of the Region II storage rack

Table I: Storage cell specification

Parameter	Value
Inter-Cell flux trap gap(cm)*	4.176
Storage cell wall material	SS304
Storage cell inner dimension(cm)	21.511
Storage cell wall thickness(cm)	0.1905
Storage cell length(cm)	425.44
Neutron absorber material	Metamic
Neutron absorber width(cm)	18.36
Neutron absorber thickness(cm)	0.27
Neutron absorber length(cm)	390.07
Distance between neutron absorbers (cm)	14.13
Fuel assembly pitch (cm)	18.66

*Region1 storage cell only.

The dimensions of the spent fuel storage racks are based on the Westinghouse AP1000 reactor spent fuel storage [1] but we adjusted the original data such that the 16x16 PLUS 7 fuel assemblies can be loaded in the rack. The thickness of the Metamic (B_4C+Al) absorber on the cell wall is 2.7 mm and this absorber is considered to reduce the reactivity. The width and axial length of this absorber are 18.36 cm and 390.07 cm, respectively. Table II summarizes the main design parameters of the PLUS 7 16x16 fuel assembly. Table III shows the initial uranium enrichments and average discharge burnups of the fuel assemblies discharged from the 6th cycle core of Hanbit Unit 3 [2] that were calculated using DeCART2D and MASTER code and, their corresponding axial burnup profiles are shown in Fig. 3.

Table II: PWR fuel assembly specifications

Parameter	Value
Fuel material	UO_2
Fuel Density(g/cm^3)	10.176
Number of fuel rods(#)	236
Fuel pin radius(cm)	0.41275
Cladding outer radius(cm)	0.48606
Cladding thickness(cm)	0.0733
Pin pitch(cm)	1.2882
Guide tube inner radius(cm)	1.4495
Guide tube outer radius(cm)	1.5513
Guide tube thickness(cm)	0.1018
Active fuel length(cm)	381
Assembly pitch(cm)	20.611
Cladding material	Zircaloy-4

Table III. Initial uranium enrichments and average discharge burnups of the discharged fuel assemblies from the 6th cycle of Hanbit Unit 3

Assembly type	Initial enrichment(wt%)	Average discharge burnup(MWD/kg)
1	4.11	51.90
2	4.40	50.14
3	4.42	50.13
4	4.31	48.40
5	4.32	48.27
6	4.08	42.60
7	4.07	42.58
8	4.03	41.76
9	4.13	41.12
10	4.50	41.06
11	4.09	40.09
12	4.07	40.06
13	3.93	39.66
14	3.93	39.64
15	3.93	39.31
16	3.85	33.92
17	3.67	33.17
18	3.68	33.16
19	3.74	31.54
20	3.74	31.51

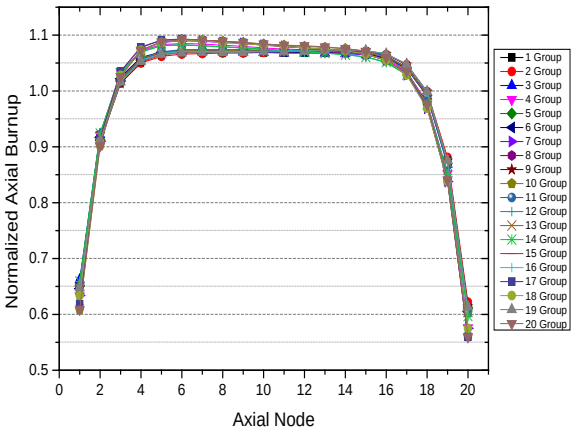

Fig. 3. Axial burnup distribution for the discharged fuel assemblies from the 6th cycle core of Hanbit Unit 3

2.2 Computational Method

In this work, the STARBUCS (Standardized Analysis of Reactivity for Burnup Credit using SCALE) sequence of SCALE6.1 was used to perform the criticality analysis with burnup credit for the spent fuel storage pool described in Sec. 2.1. The STARBUCS sequence automatizes the criticality analysis by combining the KENO V.a 3D multi-group Monte Carlo criticality and the ORIGEN-S depletion calculations in which the zone-wise depletion calculations are performed with the one-group cross section libraries [3]. The one-group cross section libraries are usually prepared with the TRITON lattice calculations. In this work, we did not consider the radial burnup distribution over the fuel pins but the axial burnup profiles given in Fig. 3. The STARBUCS sequence provides a useful function which can automatically search the initial uranium enrichment giving a specified k_{eff} with a given discharge burnup. We used this function to evaluate the loading curve for the spent fuel storage pool. In the muti-group transport calculation for estimating k_{eff} using KENO V.a, we used 600 cycles and 5000 particles for each cycle for giving statistically reliable results of k_{eff}, which gave the small standard deviation of ~40 pcm. The cross section library for multi-group transport calculation is the ENDF/B-VII 238 group cross section provided by SCALE 6.1. We applied to the reflective boundary conditions on the radial boundaries assuming infinitely repeated structure but the vacuum boundary conditions for the axial boundaries. In addition, we did not consider the burnable poison pins and the soluble boron in the coolant for conservative estimation of k_{eff}.

For burnup credit, we considered two different sets of nuclides: 1) only major actinides and 2) actinides and fission products [4]. These sets of nuclides are given in Table IV. We did not consider the cooling time except for the evaluation of the loading curves.

Table IV: Two Nuclide sets

Nuclide set 1: Major actinides only				
U-234	U-235	U-238	Pu-238	Pu-239
Pu-240	Pu-241	Pu-242	Am-241	O
Nuclide set 2: Actinides and fission products				
U-234	U-235	U-238	Pu-238	Pu-239
Pu-240	Pu-241	Pu-242	Am-241	O
Am-243	Np-237	Mo-95	Tc-99	Ru-101
Rh-103	Ag-109	Cs-133	Sm-147	Sm-149
Sm-150	Sm-151	Sm-152	Nd-143	Nd-145
Eu-151	Eu-153	Gd-155	O	

2.3 Results

The k_{eff} values obtained with only actinides in burnup credit are shown in Fig. 4. In particular, the k_{eff} values obtained with and without axial burnup profiles are also inter-compared in Fig. 4. Fig. 4 shows that all the fuel assemblies except only for four fuel assemblies (i.e., Assembly numbers 10, 16, 19, and 20) can be loaded with k_{eff} values less than 0.933. The lower bound of k_{eff} (i.e., k_{eff}=0.933) is set based on the administrative margin of 0.05 and the uncertainties including bias uncertainty of 0.0167 related only to isotopic prediction [4]. Also, the lower bound of k_{eff} should be different for the burnup credits with actinides only and actinides plus fission products but in this work we used the same values for simplicity. The exceptional four assemblies have low discharge burnups or high discharge burnups with high initial uranium enrichments. In Fig. 4, it is noted that the consideration of axial burnup profile gives lower values of k_{eff} for all the fuel assemblies.

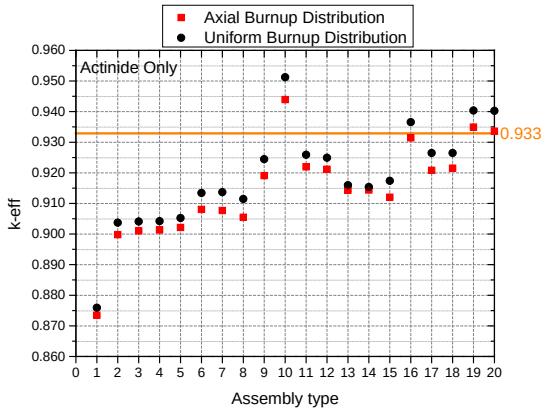

Fig. 4. Comparison of k_{eff} values obtained with and without the axial burnup (actinides only in burnup credit)

On the other hand, the k_{eff} values obtained with the actinides plus fission products in burnup credit are shown in Fig. 5. Fig. 5 shows that all of the fuel assemblies can be loaded with the application of actinides and fission products in burnup credit in the spent fuel storage pool (i.e., k_{eff} values are less than 0.933) and that the consideration of axial burnup profiles gives the larger k_{eff} values (i.e., conservative) than the one with uniform axial burnup profile, which is different from the case with consideration of actinides only.

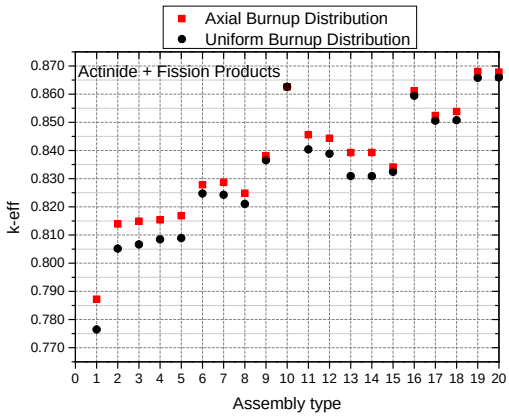

Fig. 5. Comparison of k_{eff} values obtained with and without the axial burnup (actinides and fission products in burnup credit)

The degree of the significance of axial burnup profile is usually represented in terms of the end effect which is defined as the difference in k_{eff} values between the ones obtained with and without axial burnup profiles. The end effects for all the considered fuel assemblies are shown in Figs. 6 and 7. Fig. 6 shows the end effects obtained with the burnup credit with only actinides. As shown in Fig. 6, the end effects are all negative, which means that the k_{eff} values obtained with axial burnup profile are less than the ones obtained with uniform burnup profile as shown in Fig. 4. In particular, it is noted in Fig. 6 that the end effects are large for the fuel assembly cases 6~10 and 15~20. The maximum end effect in absolute value is ~750 pcm for the case 10 assembly.

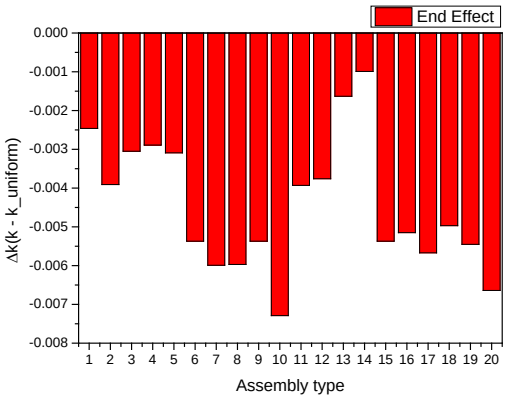

Fig. 6. Comparison of the end effects (actinides only in burnup credit)

Fig. 7 compares the end effects for the burnup credit application with the actinides plus fission products. As shown in Fig. 7, the end effects are all positive which

means that the k_{eff} values obtained with axial burnup profiles are larger than those with uniform axial burnup. In Fig. 7, it is noted that the fuel assembly cases of 1~5 and 11~14 have much larger end effects than the other cases.

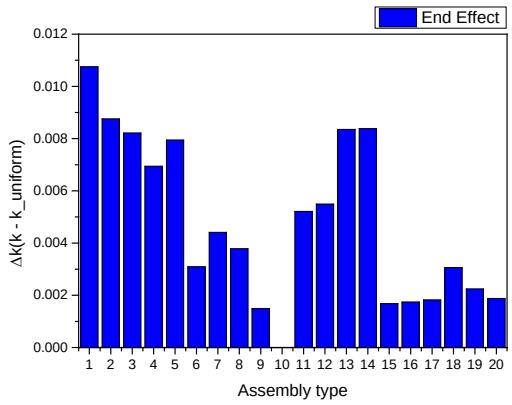

Fig. 7. Comparison of the end effects (actinides and fission products in burnup credit)

Finally, we evaluated the loading curves which guide the acceptable region for loading in burnup-initial uranium enrichment space. The loading curves were evaluated with the STARBUCS sequence to search the limiting initial uranium enrichment giving the lower bound of k_{eff} for various conditions such as different cooling times and burnup credits with only actinides and with actinides plus fission products. The obtained loading curves are plotted in Fig. 8 and the points corresponding to all the fuel assemblies discharged from Hanbit Unit 3 also are projected in Fig. 8. As expected, the consideration of actinides and fission products significantly extends the acceptable region for loading, and also the longer cooling time extends the acceptable region.

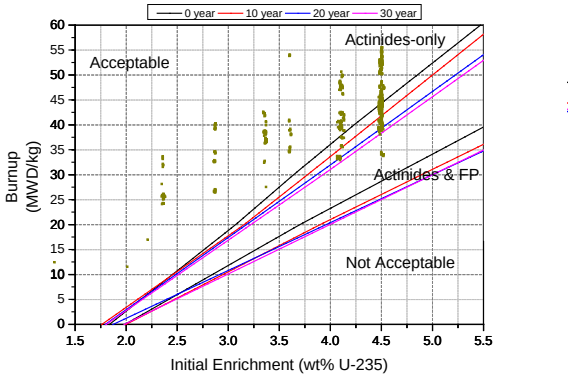

Fig. 8. Hanbit Unit 3 6th cycle loading curve.

From the loading curves, it was shown that of the projected 935 fuel assemblies discharged from Hanbit Unit 3, the numbers of acceptable fuel assemblies are estimated to be812, 902, and 927 for the cooling times of 10, 20, and 30 years, respectively.

3. Conclusion

In this work, the extensive study of the criticality analysis was performed with STARBUCS sequence of SCALE 6.1 for evaluating the end effects and the loading curves of the PWR spent fuel storage pool. From the results of the analysis, it was shown that the end effects with the burnup credit with only actinides are all negative while the ones with the actinides and fission products are all positive with the axial burnup profiles obtained with the reload core follow calculations. For the spent fuels discharged from the 6th cycle of Hanbit Unit 3, all of them can be loaded with the burnup credit in actinides and fission products, and even without consideration of the cooling time. As expected, the consideration of actinides and fission products in burnup credit significantly extends the acceptable region in comparison with the cases with only actinides in burnup credit. Also, we estimated the acceptable spent fuel assemblies through the projection of all the discharged fuel assemblies from Hanbit Unit 3 on the loading curves. However, the evaluation of the loading curves depends on the uncertainties of isotopic estimation and cross sections and so we will perform the future work to estimate the lower bound of k_{eff} with more precise estimation of the uncertainties.

ACKNOWLEDGEMENTS

This work was supported by KOERA HYDRO & NUCLEAR POWER CO., LTD (No. 20180291) and partially supported by “Human Resources Program in Energy Technology” of the Korea Institute of Energy Technology Evaluation and Planning (KETEP), granted financial resource from the Ministry of Trade, Industry & Energy, Republic of Korea. (No. 20164030200990)

REFERENCES

[1] Westinghouse Electric Company LLC, AP1000 Standard Combined License Technical Report Spent Fuel Storage Racks Criticality Analysis, APP-GW-GLR-029, 2006.
[2] Hyungju Yun, Do-Yeon Kim, Kwangheon Park, and Ser Gi Hong, A Criticality Analysis of the GBC-32 Dry Storage Cask with Hanbit Nuclear Power Plant Unit 3 Fuel Assemblies from the Viewpoint of Burnup Credit, Nuclear Engineering and Technology, Vol. 48, pp. 624-634, 2016.
[3] G. Radulescu and I. C. Gauld, STARBUCS: A Scale Control Module for Automated Criticality Safety Analyses Using Burnup Credit, ORNL/TM-2005/39 Version 6.1, Section C10, 2011.
[4] G. Radulescu, I. C. Gauld, G. IIas, and J. C. Wagner, An Approach for Validating Actinide and Fission Product Burnup Credit Criticality Safety Analyses-Isotopic Composition Predictions, NUREG/CR-7108, ORNL/TM-2011/509, 2012.